

Date of publication xxxx 00, 0000, date of current version xxxx 00, 0000.

Digital Object Identifier 10.1109/ACCESS.2024.Doi Number

Efficient Approach for Brain Tumor Detection and Classification Using Fuzzy Thresholding and Deep Learning Algorithms

Nashaat M. Hussain Hassan^{*1, 2}, Wadii Boulila³

¹Faculty of Engineering and Technology, Badr University in Cairo (BUC), Cairo, Egypt

²Electronics and Communication Engineering Dept, Fayoum University, Fayoum, 63514, Egypt

³Robotics and Internet-of-Things Laboratory, Prince Sultan University, Riyadh 12435, Saudi Arabia

Corresponding author: Nashaat M. Hussain Hassan (e-mail: nmh01@fayoum.edu.eg).

ABSTRACT Accurate and efficient brain tumor diagnosis remains a critical challenge in medical imaging. This study proposes a novel framework that integrates fuzzy logic-based segmentation with deep learning (DL) techniques to enhance brain tumor detection and classification in magnetic resonance imaging (MRI) scans. In the first stage, a fuzzy thresholding approach is applied to segment MRI images into healthy and abnormal regions, enabling the precise extraction of tumor areas. In the second stage, an optimized convolutional neural network (CNN) model classifies tumors into four categories: glioma, meningioma, pituitary tumor, and no tumor. The proposed method is evaluated across three large public datasets comprising more than 23,000 MRI images. Experimental results demonstrate that the model achieved an accuracy of 98% and a Dice similarity coefficient of 97.97%, confirming its high effectiveness in accurately extracting tumor regions and classifying them correctly. Furthermore, the proposed system outperforms conventional machine learning, deep learning, and transfer learning techniques. In addition to classification, the system accurately estimates tumor size, providing valuable clinical insights. These findings highlight the potential of combining fuzzy logic with DL to improve automated brain tumor diagnostics, enhance diagnostic reliability, and support clinical decision-making.

INDEX TERMS Brain tumor extraction; fuzzy logic; brain tumor size calculation; tumor segmentation; deep learning; magnetic resonance imaging

I. INTRODUCTION

Over the past three decades, brain tumor cancer has affected more than fourteen million individuals worldwide [1]. These malignancies represent a significant cause of mortality globally due to their aggressive nature and profound impact on neurological function. Despite advances in medical care, epidemiological projections suggest that the global incidence of brain tumors may rise to twenty-one million cases by 2030, highlighting the urgent need for improved prevention strategies and treatment protocols that align with sustainable healthcare development goals. Although the chances of effective treatment for various tumors increase significantly with early detection and timely intervention, it is currently estimated that 30% to 50% of cancer cases could be prevented through early recognition of the disease [2]. The economic impact of cancer is significantly reduced through early detection, enabling patients to continue working and supporting their families while also saving substantial costs on treatment. Professionals diagnose brain cancers manually, but this process is very challenging. It is time-consuming for many experts, and the results can vary significantly. Even diagnoses made by the same physician under different conditions can result in inconsistent outcomes. Furthermore,

variations in screen contrast and illumination can affect the accuracy of tumor detection. These factors highlight the importance of automated brain tumor identification [3], which can improve diagnostic consistency and enhance patient recovery prospects. Consequently, numerous studies aim to develop methods for rapid and accurate tumor identification while minimizing the reliance on manual effort. Machine learning (ML) advancements [4] have provided radiologists with new perspectives for interpreting magnetic resonance (MR) images, enhancing both recognition and classification [5]. Diagnostic imaging methods [6] are considered to be highly dependable and frequently used for identifying cancer in various types, along with their ability to recognize tumors. Diagnostic imaging methods [6], such as magnetic resonance imaging (MRI), are commonly used due to their offering of distinct images of brain cells that aid in the diagnosis and categorization of various brain cancers. Brain cancers vary widely in terms of their density levels, shapes, and dimensions [7]. Tumors with different pathological characteristics might also seem the same. The application of neural network algorithms to the extensive dataset of magnetic resonance images (MRI) posed significant challenges, primarily due to the large data volume

and the inherent variability within the images. However, utilizing all the available MR images could expand the collection because they are acquired on several planes. Proper preparation of magnetic resonance (MR) images is crucial to ensure accurate classification outcomes when using different neural networks [8]. Convolutional neural networks (CNNs) addressed this problem [9], offering the advantages of automatic feature enhancement and requiring less extensive data preparation. Using simpler networking requires fewer facilities for setup and retraining.

Computer-assisted diagnosis (CAD) of brain tumors is one of the topics that receive significant attention from researchers for many reasons, including the gravity of the disease and its spread, the critical importance of early detection and identification, the accurate identification of the different locations, no matter how small they are, and determining the size of the tumor. Accurately and rapidly classifying tumor types without errors or the need for extensive, time-consuming, and costly testing remains a critical objective. This also relieves the patient from waiting for a long time to meet the doctor, as well as traveling, which may often be from faraway places. This is in addition to saving time and effort and ensuring the accuracy of the decision regarding the doctor [10-11]. After reviewing several scientific publications on the use of DL techniques for extracting and classifying brain tumors, several important observations were made. Much of the existing literature exhibits certain limitations, including the lack of large and diverse datasets, insufficient use of varied evaluation mechanisms to validate the effectiveness of proposed techniques, and an absence of detailed reporting on processing speeds. Furthermore, many studies focus solely on improving classification accuracy without addressing critical aspects such as tumor size, severity, or comparisons with the most recent state-of-the-art methodologies. All these observations were taken into consideration in the study presented in this work. Our proposed approach is based on the combination of fuzzy logic and improved DL techniques to extract and classify brain tumors with excellent accuracy, maximum speed, and lowest implementation cost through two innovative approaches. The first step, which is dedicated to extracting tumors, relies on using the fuzzy controller [12] first to calculate the threshold value and second to divide the images into two regions: tumor-free regions or regions containing tumors. The second method is dedicated to classifying brain tumors into four classes. The second step relies on using an improved DL technique [13]. To verify the efficiency of the proposed techniques, the results were compared with the results of several related techniques (ML, DL, and TL techniques). The results showed a significant advantage in favor of the proposed techniques, which enhances the chances of using these techniques in real applications.

The structure of this work is organized as follows: An overview of previous studies on identifying and categorizing brain tumor detection and classification is included in Section 2. The suggested process for locating and

categorizing brain tumors is described in Section 3. The test results of the suggested technique are then thoroughly compared to those of comparable methods, and these results are analyzed. The conclusion and recommendations for additional study are provided at the end.

II. Literature Review

It is difficult to categorize brain tumors into distinct groups. The ability of magnetic resonance imaging (MRI) to identify and categorize brain cancers has been the focus of multiple investigations utilizing diverse techniques. Sasikala et al. [14] employed a neural network for classification, utilizing wavelet-based feature extraction followed by feature selection with a genetic algorithm (GA) to identify relevant brain tumor characteristics. Similarly, El-Dahshan et al. [15] proposed a multi-stage classification approach: they first extracted features using the discrete wavelet transform (DWT), then reduced dimensionality using principal component analysis (PCA), and finally performed classification using either a feedforward backpropagation artificial neural network (FP-ANN) or a K-nearest neighbor (KNN) classifier based on the reduced feature set. Local Binary Pattern (LBP), nLBP, and α LBP were the three different approaches used by Kaplan et al. [16] for acquiring features. KNN, ANN, Random Forest (RF), AIDE, and LDA (Linear Discriminant Analysis) methods were used for the categorization procedure; KNN and nLBPd=1 provided an overall achievement rate, of 95.56%. The categorization method was mainly implemented by Rathi and Palani [17], utilizing kernel-based probability clustering methods on noise-free images that had been processed via median filtering. For brain tumor classification, deep learning techniques were applied with linear discriminant analysis to evaluate key features extracted from each data segment. Mohsen et al. [18] investigated the application of deep neural networks (DNNs) for brain tumor classification, contributing to the growing body of research in this domain. The researchers utilized 66 MRI scans of the human brain to assess the DNN-based categorization framework, as well as analysis of principal components and discrete wavelet transformation methods to derive attributes. In 2015, Cheng [19] developed a brain tumor dataset to address the three-class brain tumor classification problem. Their methodology involved feature extraction using brightness histograms, gray-level co-occurrence matrices, and bag-of-words models, followed by tumor region enhancement through image dilation. Support Vector Machines (SVMs) were then employed for classification, achieving a maximum accuracy of 91.28%. Pashaei et al. [20] used CNN and Kernel Extreme Learning Machines (KELM) to classify brain tumors, achieving a 93.68% efficiency rate. In [21], Phaye et al. used different capsule structures to classify brain tumors. By substituting highly linked layers of convolution for the typical convolution phase in the CapsNet, this approach raised the precision to 95.03%. A team of researchers [22] presented their research approach consisting of using CNN to recognize brain cancers from MRI images, achieving 96.56% accuracy. A DNN design with two distinct channels

has been suggested by J. D. Bodapati et al. [23]. A variety of feature extraction methods, such as pre-trained CNN blocks as well as the attention system, are employed in the classification of MRI brain cancers. Compared to other classifiers employed in similar investigations, the classifier's precision rate of 98.04% was greater. Three CNN architectures were combined into an arrangement by A. Rehman et al. [24], and the resulting VGG16 model achieved 98.69% efficiency. S. Deepak et al. [25] proposed a multi-label categorization approach to use brain MRI data to diagnose cancers in patients. Using GoogleNet pre-trained mode, the author extracted the features, and the proposed method achieved an average accuracy of 98%.

The integration of fuzzy systems with DL algorithms for the detection and classification of human brain tumors has emerged as a significant research trend in recent years. The following is a review of some of these literature studies. To achieve a binary categorization of brain tumors, Narasimham et al. [26] suggested using fuzzy logic. Experiments were conducted on 253 MRI scans. An efficiency of 96% was attained in this study. Despite its high efficiency, this work has been tested on a limited dataset of only 253 images. Furthermore, unlike our proposed study, the work of Narasimham et al. uses a binary classification and does not classify the various forms of brain tumors. Additionally, the findings of this study were not contrasted with those of other comparable works. Pham et al. [27] proposed an approach combining CNN and fuzzy logic methods. In this study, the tumor was classified using CNN following a segmentation using fuzzy logic. This study was limited by a small dataset of 394 MRI images, which poses a challenge despite achieving a high detection and classification efficiency of 97.6%. Moreover, the study did not measure the tumor size and only determined whether an image was healthy or contained a tumor. Maqsood et al. [28] combined fuzzy logic and U-Net CNN to extract brain tumors, achieving an efficiency rate of 98%. While this approach proved highly effective, the study had certain limitations. It relied on a relatively small dataset of 1,134 MRI images, which may affect the reliability of the results. Additionally, the study did not calculate tumor size, even though its primary focus was tumor extraction rather than classification. Murthy et al. [29] suggested a method to perform binary classification for human brain tumors based on the Fuzzy system and CNN. After the tumor was segmented, the authors used the Optimized Convolutional Neural Network with Ensemble Classification (OCNN-EC) in conjunction with Adaptive Fuzzy Deformable Fusion (AFDF)-based segmentation. The dataset used in this study only included 155 MRI images, which were separated into normal and abnormal images. Despite achieving a high accuracy of 96%, the approach used in this study has several limitations. First, it relies on a very small dataset of only 155 images, which raises concerns about the reliability of the results. Additionally, this method is limited to classifying images into only two categories (normal and abnormal), a task that can be accomplished using more conventional techniques. Furthermore, the study

did not provide information on processing time or its feasibility for real-world applications.

After reviewing several scientific studies on DL techniques for brain tumor extraction and classification, we can conclude that while significant progress has been made in detecting and categorizing brain tumors, most studies tend to focus on a single aspect rather than adopting a comprehensive and multi-dimensional approach. Although several studies have highlighted significant advancements in brain tumor detection and classification methods, most of them have limitations. Many fail to adopt a comprehensive approach, focusing on a single aspect rather than examining the subject from multiple perspectives. Another limitation is the reliance on relatively small datasets, which may affect the reliability of the results. Additionally, many studies do not incorporate a diverse set of evaluation metrics, making it difficult to fully validate the effectiveness of their proposed techniques. This is in addition to the fact that most of these studies do not mention the processing time for the recommended solutions, which is not helpful to these methods. This study proposes an approach that enhances brain tumor analysis by combining high-resolution tumor extraction, precise tumor size calculation, and highly efficient classification of brain tumor MRI images into four categories. Additionally, it ensures the use of a large and diverse dataset to enhance reliability. Moreover, multiple evaluation metrics are employed to comprehensively assess the effectiveness of the proposed methods. Table 1 summarizes the advantages and disadvantages of the most important studies published on this topic in the last two years (2023-2024).

This study explores the use of fuzzy logic and DL algorithms to enhance the accuracy and speed of brain tumor extraction and classification. The process begins with tumor extraction, where a fuzzy controller determines the appropriate threshold value and segments MRI images into two categories: tumor and non-tumor regions. In the next step, a DL-based approach is applied to classify brain tumors into four distinct categories. To evaluate the effectiveness of the proposed methods, the results were compared with other techniques, including machine learning (ML), DL, and transfer learning approaches. The findings demonstrated significant advantages, suggesting that the proposed methods have promising potential for practical application.

III. PROPOSED METHODOLOGY

This study aims to explore the diagnostic application of artificial intelligence and digital image processing techniques for detecting brain tumors. The proposed approach is based on three stages. The aim of the first stage is to extract brain tumor regions using fuzzy thresholding. The second stage calculates the size of the brain tumor. The last stage divides the dataset into three subsets: training, validation, and testing. Figure 1 provides a visual representation of the proposed approach.

The first stage includes three steps: database collection, MRI image preprocessing, and brain tumor extraction. The second stage involves calculating the size of the tumor. The final stage consists of dividing the database into three subsets: training, validation, and testing. This stage also includes training and validating the proposed CNN classifier, fine-tuning hyperparameters, and evaluating its performance on the test set. Each of these processes is explained in detail in the following sections.

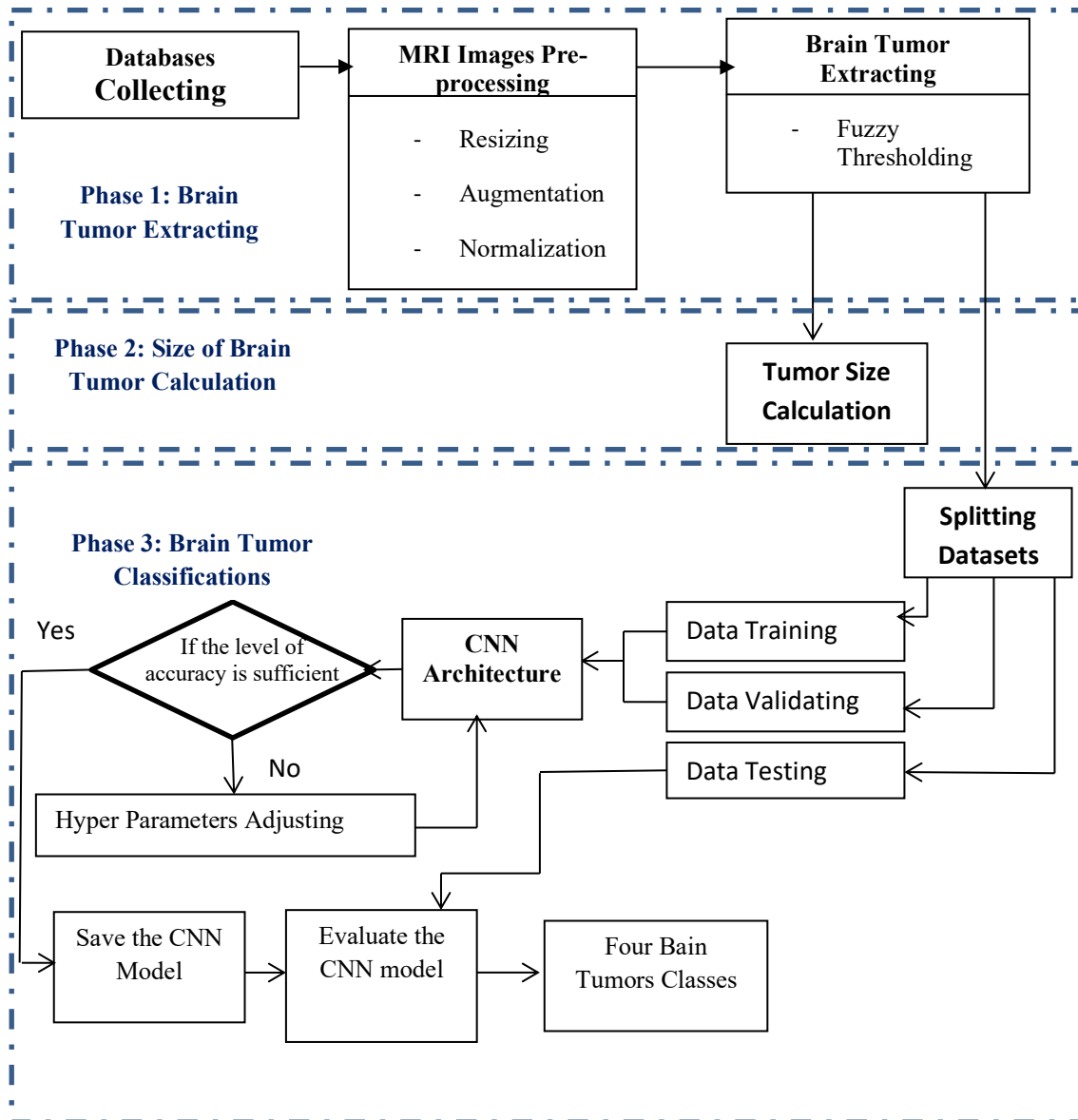


Figure 1. The general architecture of the proposed approach

TABLE 1
BENEFITS AND DRAWBACKS OF THE MOST SIGNIFICANT RESEARCH ON THIS SUBJECT THAT HAS BEEN PUBLISHED IN THE LAST TWO YEARS

Refer ences	Public ation Year	Technique	Pros	Cons
[30]	2023	Automated brain tumor detection and segmentation for treatment response assessment using Amino Acid PET	<p>1-The accuracy of the proposed technique has achieved 93%</p> <p>2-The study was conducted on a database consisting of images extracted by modern imaging systems (based on amino acid PET)</p> <p>3-Relying on deep learning techniques</p>	<p>1. The study relied on the use of only 699 amino acid PET scans</p> <p>2. The study did not provide details about the computation times of the proposed technique</p> <p>3. The study presented a method that only deals with measuring changes in tumor size. This was explored by many existing techniques</p> <p>4. Accuracy can be improved.</p> <p>5. This study did not focus on determining the size or type of defect</p>
[31]	2024	Brain tumor detection using MRI and convolutional neural networks	<p>1-The study was conducted on a large database of 300,000 MRI images</p> <p>2-The proposed technique provides a high efficiency of 97%</p> <p>3-Use of DL techniques</p>	<p>1. There are just two types that this study separates: healthy and tumors. This was explored by many existing methods</p> <p>2. The outcomes of the method have not been contrasted with similar related methods</p> <p>3. This study did not focus on determining the size or type of defect</p>
[32]	2024	Brain tumor detection and classification using transfer learning models	The study presents a technique for classifying brain tumors into four categories based on transfer learning techniques, achieving a high accuracy of 99%.	<p>1. The study was based on an average database consisting of 3264 MRI images</p> <p>2. There was no significant difference between the results of the accuracy of the performance of the technique presented in this study and the results of the three techniques. Computation times of the technique were not mentioned</p> <p>3. The size of the tumor and its degree of severity were not mentioned.</p>
[33]	2024	Brain tumor detection and classification in MRI using hybrid ViT and GRU model	1-This study was related to improving the identification and categorization of brain cancers	<p>1. The study was conducted on a small database of 1166 MRI scans.</p> <p>2. The study proposed to separate only two categories (normal and abnormal MRI images). Many existing research</p>

		with explainable AI in Southern Bangladesh	in MRI scans by merging the Gated Recurrent Unit (GRU) and Vision Transformer (ViT) algorithms into a novel approach 2-The model achieved precision, recall, and F1-score metrics of 97%.	works have achieved similar results 3. The size of the tumor and its degree of severity were not mentioned 4. Computation times of the technique presented were not mentioned
[34]	2023	Classification of brain tumor images using CNN	1-The study presented a method that achieves high-performance accuracy 2- The proposed technique demonstrates an advantage in processing time compared to the technique it was evaluated against	1. The database used in this study is very small; it does not exceed 253 images 2. The results of the test of the technique presented in this study were only compared with the results of one test technique, which is VGG16 3. The technique presented in this study only classifies between two categories (MRI normal, MRI with tumor). 4. The technique presented in this study did not mention computation time and the tumor size
[35]	2024	Brain tumor detection and classification using an optimized CNN	1-The technique presented in this study used three databases with a total number of MRI images of 7562 2-The technique presented in this study classified four types of brain tumors 3-The average performance accuracy of the technique presented in this study was 95.33%	1. The results were very close between the technique presented in this study and related techniques 2. The technique presented in this study did not mention computation time and the tumor size

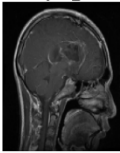
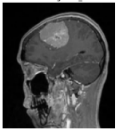
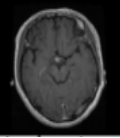
A. DATABASE COLLECTION

To verify the efficiency of the proposed technique, three different databases have been considered, including MRI images from diverse sources and under varied conditions. This section discusses the details of each one of them Table

2 shows a description of the first database used in this study. The dataset contains 3264 MRI images divided into two folders: the first contains 2870 MRI training images (826 glioma tumors, 822 meningioma tumors, 395 no-tumor, and

827 pituitary tumors), and the other contains 394 MRI test images (100 glioma tumors, 115 meningioma tumors, 105 no-tumor, and 74 pituitary tumors). This dataset is available for free online at [36]. Table 3 shows a description of the second dataset which was used in our proposed study. The dataset contains 7023 images of human brain MRI images which are classified into four classes (glioma- meningioma- no tumor- and pituitary). This dataset is divided into two folders, the first contains training images which included 5712 MRI images (1321 glioma tumors, 1339 meningioma tumors, 1595 no-tumor, and 1457 pituitary tumors), and the other contains test images which included 1311 MRI images (300 glioma tumors, 306 meningioma tumors, 405 no-tumor, and 300 pituitary tumors). This dataset is available for free online at [37]. The description of the last dataset used in our proposed study is shown in Table 4. This dataset consists of MRI scans of brain tumors and has a total of 13352 images of 4 classes: glioma, meningioma, pituitary, and no tumor. The dataset consists of 3 different datasets that were merged to form a larger dataset. The dataset was published by Jun Cheng on December 21, 2024, at 04:57. This dataset is split into two folders, the first contains training images which included 10681 MRI images (3179 glioma tumors, 2632 meningioma tumors, 2000 no-tumor, and 2870 pituitary tumors), and the other contains test images which included 2671 MRI images (795 glioma tumors, 658 meningioma tumors, 500 no-tumor, and 718 pituitary tumors). This dataset is available for free online at [38]. These 23639 images are all MRI scans of the human brain. They depict four various types of brain tumors in people. There are various sizes available for these images and they are freely accessible online. The data distribution of the considered datasets is shown in Figure 2.

TABLE 2
AN OVERVIEW OF THE FIRST DATASET

Class Name	Total	Trainin g Images	Testin g Ima ges	Samples
Glioma Tumors	926	826	100	
Meningiomas Tumors	937	822	115	
No Tumors	500	395	105	

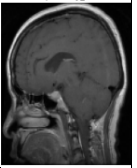
Pituitary Tumors	901	827	74	
Total MRI Images	3264	2870	394	

TABLE 3
AN OVERVIEW OF THE SECOND DATASET

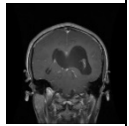
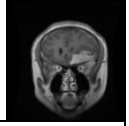
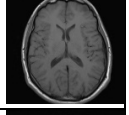
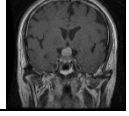
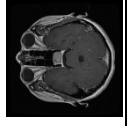
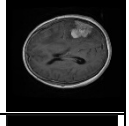

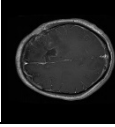
Class Name	Total	Trainin g Imag es	Testin g Image s	Samples
Glioma Tumors	1621	1321	300	
Meningiomas Tumors	1645	1339	306	
No Tumors	2000	1595	405	
Pituitary Tumors	1757	1457	300	
Total MRI Images	7023	5712	1311	

TABLE 4
AN OVERVIEW OF THE THIRD DATASET

Class Name	Total	Trainin g Images	Testin g Image s	Samples
Glioma Tumors	3974	3179	795	
Meningiomas Tumors	3290	2632	658	
No Tumors	2500	2000	500	

Pituitary Tumors		2870	718	
	3588			
Total MRI Images	13352	10681	2671	

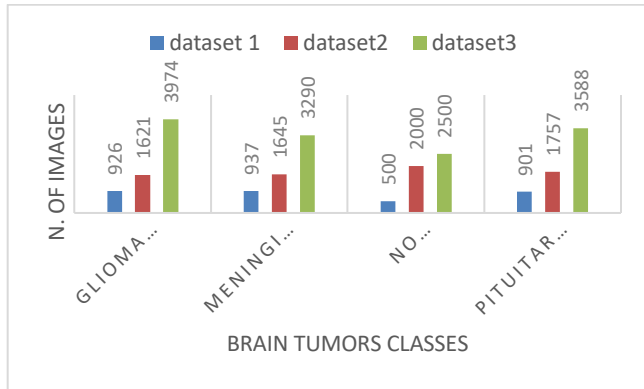


Figure 2. Distribution of the three different databases used in our proposal

B. MRI IMAGES PRE-PROCESSING

The collection of data is initially resized into MRI images with a size of 250 by 250. This serves to test our theory. Along with shrinking the images, feature scaling method also included normalizing the collected dataset. The CNN model operates faster when input data is normalized to the [0,1] range compared to the original [0,255] scale. In the presented study, data augmentation was proposed as the third step in preprocessing the gathered data, with the aim of enhancing the diversity and size of the dataset used, which helps to prevent overfitting and improve the generalization ability of the machine learning model. Four distinct degrees of rotation were applied to all the data that was gathered: 0°, 90°, 180°, and 270°. After augmentation, each dataset's class of images was quadrupled as shown in Figure 3. These images were then split into three groups for training, validation, and testing with 80% for training, 10% for validation, and 10% for testing.



Figure 3. Dataset distribution after augmentation

A selection of our augmented phase results is shown in Table 5. The following list includes several mathematical formulas for the preparation activity that are employed:

- For resizing images:
 - If the original image's width and height are equal, then:

$$\text{new_width} = \text{old_width}/r \quad \text{where } r \text{ is } > 1 \quad (1)$$

$$\text{new_height} = \text{old_height}/r \quad \text{where } r \text{ is } > 1 \quad (2)$$
 - If the original image's width and height are different, then:

$$\text{new_width} = \text{square_root}((\text{original_width} / \text{original_height}) \times \text{target_area}) \quad (3)$$

$$\text{new_height} = \text{target_area} / \text{new_width} \quad (4)$$

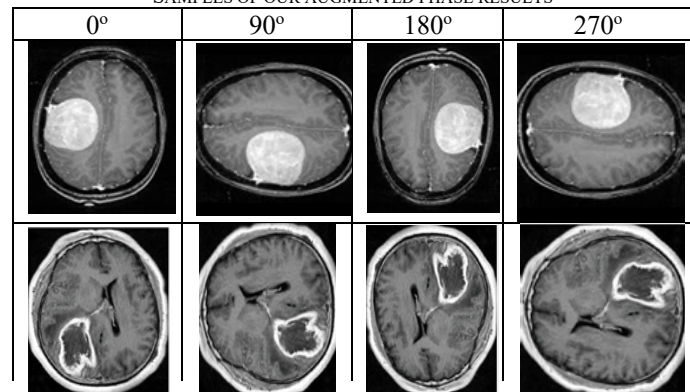
In which target area is determined by

$$\text{Target_area} = \text{original_width} * \text{original_height} \quad (5)$$

- To normalize images:

$$\text{Imgout}(i, j) = \text{imgin}(i, j) * (1/255) \quad (6)$$

TABLE 5
SAMPLES OF OUR AUGMENTED PHASE RESULTS



C. BRAIN TUMOR DETECTION

Two factors motivate the interest in tumor area extraction in this study. The first motivation was to reduce the amount of time needed to detect tumor regions. Second, the size and level of risk associated with the tumor are determined. Our proposed method to detect the tumor region is based on applying fuzzy logic. It consists of two phases: first, calculate a threshold value using fuzzy thresholding; second, segment the different regions of the MRI images based on applying the fuzzy controller. The suggested approach is explained in the following sections.

1) THRESHOLD VALUE CALCULATION

Classifying pixels into two different groups (black and white) is possible with approaches built around thresholding images. To differentiate image objects from the backgrounds, the following adjustment is applied. A limit called T is used to compare the values of every pixel created

in this binary image; any value below the threshold is regarded as an object, while values over the threshold are part of the background. Accordingly, if the image's pixel set is G :

$$G = \{0, 1, \dots, L-1\} \begin{cases} 0 & \text{black} \\ L-1 & \text{white} \end{cases}$$

To make the subsequent transformation, an upper limit $T \in G$ is established.

$$y_{i,j} = \begin{cases} 0 & \text{if } x_{i,j} < T \\ L-1 & \text{if } x_{i,j} > T \end{cases} \quad (7)$$

When $y_{i,j}$ is the pixel that corresponds to the binary image, and $x_{i,j}$ is a pixel from the original image. To choose the threshold value T , there are multiple options. The most popular techniques for calculating thresholds depend on histogram analyses [39]. These techniques for calculating the threshold value depend on counting the number of times each level is repeated. Therefore, it requires reading the image 256 times in order to calculate the number of times 256 levels are repeated. This will incur significant costs for hardware implementation. Therefore, the proposal is to rely on fuzzy logic to calculate the best value for the threshold after reading the image only once. The suggested method is predicated on using fuzzy logic to determine the threshold T . According to an analytical perspective, this method just involves computing the mean that is subsequently fitted to the image's distribution. One benefit of using this approach is that the computation methodology speeds up the processing cycle because it simply requires analyzing the image one time. This makes it possible to determine the threshold value directly, which may result in reducing the cost of hardware realization. Each pixel that will be analyzed is fed into the fuzzy technique's inputs, and the consequence represents the outcome of the fuzzy inferences. Following the MRI image reading, the outcome displays its threshold T value. Essentially, the process that creates the fuzzy structure is equivalent to using the formula that follows to calculate the image's histogram's center of weight as follows:

$$T = \frac{\sum_{i=1}^M \sum_{j=1}^R \alpha_{ij} c_{ij}}{\sum_{i=1}^M \sum_{j=1}^R \alpha_{ji}} \quad (8)$$

In which T is the value of the threshold, M indicates the image's pixel count, R represents the fuzzy mechanism's total number of rules, c denotes the rules subsequently, and α provides the rule's activation degrees. The universe of discourse of the histogram is divided into a collection of N with equal distribution membership functions to perform the fuzzy inference. A partition for $N = 16$ is proposed in our planned method (from U_1 to U_{16}) as shown in Figure 4. Since triangular membership functions are simpler to accomplish via hardware, they have been utilized.

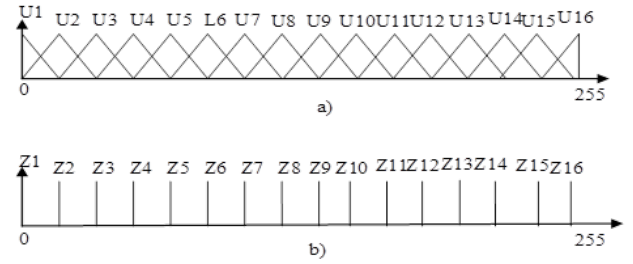


Figure 4. Functions of membership (a) antecedents (from U_1 to U_{16}) and (b) consequents (from Z_1 to Z_{16}) for $N = 16$

Within the histogram's discourse universe, the membership functions forming the consequence (from Z_1 to Z_{16}) have equal distributions of singleton functions. The utilization of singleton-type membership functions for the consequence permits the application of defuzzification techniques that are made simpler, including the fuzzy mean. The membership functions specified in Figure 4 served as the fundamental basis for the framework depicted in Figure 4, which follows. Since the rule base (rule base and membership functions) is universal for all images, the parameters can be easily stored in ROM storage.

As shown in Figure 5, the proposed fuzzy controller module to calculate the threshold value consists of 16 fuzzy rules. There will be 16 distinct values in each of the 16 groups created by splitting the image histogram. If a pixel belongs to a group, its value will be equal to the group's value. For instance, the value of the pixel will take the value of the first group if its value is in the first group, and so on.

```

if U is U 1 then Z is Z 1;
if U is U 2 then Z is Z 2;
if U is U 3 then Z is Z 3;
if U is U 4 then Z is Z 4;
if U is U 5 then Z is Z 5;
if U is U 6 then Z is Z 6;
if U is U 7 then Z is Z 7;
if U is U 8 then Z is Z 8;
if U is U 9 then Z is Z 9;
if U is U 10 then Z is Z 10;
if U is U 11 then Z is Z 11;
if U is U 12 then Z is Z 12;
if U is U 13 then Z is Z 13;
if U is U 14 then Z is Z 14;
if U is U 15 then Z is Z 15;
if U is U 16 then Z is Z 16;

```

Figure 5. Proposed rule base for $N=16$

If the model recommended has been normalized, the formula given in issue (8) can be optimized. The total extended to the rule base of the consequent's activation degrees in this instance bears value 1:

$$\sum_{i=1}^R \alpha_{ij} = 1$$

After that, formula (8) becomes:

$$T = \frac{1}{M} \sum_{i=1}^M \sum_{j=1}^R \alpha_{ij} c_{ij} \quad (9)$$

Figure 6 shows the different values assigned to the antecedents and the consequences according to the proposal presented in this study. It is important to keep in mind that the medium value is the ideal one to give each group. For instance, group 2 was given the value 16 because it spans the range 0 to 32, and so on. It's important to note that splitting

the image's histogram into 16 membership functions produced better results than splitting it into 8, as this allowed for a finer representation of intensity variations, which led to a more accurate calculation of the threshold value and improved the performance of extracting brain tumors.

```
a=addvar(a,'input','U',[0,255]);
a=addvar(a,'input','U1,trimf',[0 0 16]);
a=addvar(a,'input','U2,trimf',[0 16 32]);
a=addvar(a,'input','U3,trimf',[16 32 48]);
a=addvar(a,'input','U4,trimf',[32 48 64]);
a=addvar(a,'input','U5,trimf',[48 64 80]);
a=addvar(a,'input','U6,trimf',[64 80 96]);
a=addvar(a,'input','U7,trimf',[80 96 112]);
a=addvar(a,'input','U8,trimf',[96 112 128]);
a=addvar(a,'input','U9,trimf',[112 128 144]);
a=addvar(a,'input','U10,trimf',[128 144 160]);
a=addvar(a,'input','U11,trimf',[144 160 176]);
a=addvar(a,'input','U12,trimf',[160 176 192]);
a=addvar(a,'input','U13,trimf',[176 192 208]);
a=addvar(a,'input','U14,trimf',[192 208 224]);
a=addvar(a,'input','U15,trimf',[208 224 255]);
a=addvar(a,'input','U16,trimf',[224 255 255]);
a) MF for antecedents
```

```
a=addvar(a,'output','Z',[0 255]);
a=addmf(a,'output',1,'Z1','sinimf',[0]);
a=addmf(a,'output',1,'Z2','sinimf',[16]);
a=addmf(a,'output',1,'Z3','sinimf',[32]);
a=addmf(a,'output',1,'Z4','sinimf',[48]);
a=addmf(a,'output',1,'Z5','sinimf',[64]);
a=addmf(a,'output',1,'Z6','sinimf',[80]);
a=addmf(a,'output',1,'Z7','sinimf',[96]);
a=addmf(a,'output',1,'Z8','sinimf',[112]);
a=addmf(a,'output',1,'Z9','sinimf',[128]);
a=addmf(a,'output',1,'Z10','sinimf',[144]);
a=addmf(a,'output',1,'Z11','sinimf',[160]);
a=addmf(a,'output',1,'Z12','sinimf',[176]);
a=addmf(a,'output',1,'Z13','sinimf',[192]);
a=addmf(a,'output',1,'Z14','sinimf',[208]);
a=addmf(a,'output',1,'Z15','sinimf',[224]);
a=addmf(a,'output',1,'Z16','sinimf',[255]);
```

b) MF for consequents

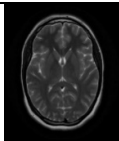
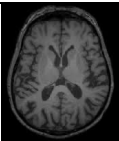
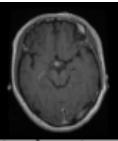
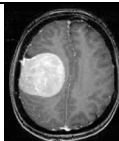
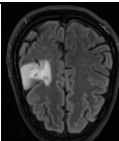
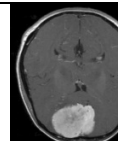
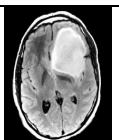
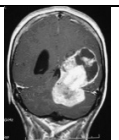
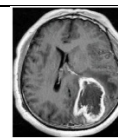
Figure 6. Membership functions of the proposed Fuzzy inference model, a) MF for Antecedents, b) MF for consequents

2) MRI HUMAN BRAIN SEGMENTATION

When examining MRI images of the human brain, one can observe that brain masses that are consistent with one another are a sign of a healthy brain. There are no regions in it that are distinct from the remainder of the brain. However, as Table 6 illustrates, images of patients with brain tumors demonstrate that the cerebral mass is not uniform because one or more areas are present that are entirely distinct from the rest of the cerebral mass. When these spots are examined in greater detail and contrasted with the remaining brain

mass, it becomes clear that the unaffected brain mass area has lighting that is neither low nor high, whereas the spots' areas have lighting that is either significantly higher or much lower than that of the healthy areas. From this standpoint, a proposal is presented based on the use of a fuzzy controller theory to extract all areas containing tumors, no matter how small, without considering healthy areas. The proposal is based on dividing the histogram of the image into three regions: a region with low illumination intensity, a region with medium illumination intensity, and a region with high illumination intensity.

TABLE 6
SEGMENTATION OF MRI BRAIN TUMORS ACCORDING TO THE DEGREE OF HOMOGENEITY OF THE BRAIN MASS

Classes		MRI of Human Brain Images		
No_Tumor(Complete homogeneity)				
Yes_Tumor	Yes_Tumor_or_with only one Spot (Partial heterogeneity)			
	Yes_Tumor_or_with more than one Spot (Complete heterogeneity)			

The proposed fuzzy inference controller module is based on dividing the histogram of the MRI image into five regions (an area with very low light intensity, an area with low intensity, medium, high, and an area with very high light intensity). Therefore, the universe of discourse of the antecedents of the proposed fuzzy controller module consists of five triangular membership functions that are not equally spaced with an overlapping degree of two (Very Low (VL), Low (L), Medium (M), High (H), and Very High (VH), as shown in Figure 7-a. The universe of discourse of the output of the proposed fuzzy inference module consists of five singleton functions, and the different values of the five functions as shown in Figure 7-b. The proposed fuzzy controller module consists of five fuzzy rules, as shown in Figure 7-c. These rules, as shown in the

figure, were built based on the following: If the pixel is found in area VL or VH, it is classified as a tumor area and takes the value 255, while if it is found in area M, it is classified as a normal area (not a tumor area). However, if the pixel is found in area L or H, it is possible that it may be a tumor, and it may also not be so. Therefore, to determine this, if the pixel is found in the L area, the question is asked whether the value of the pixel is closer to VL than M, then it is classified as a tumor and vice versa. If the pixel is found in area H, then the question is asked whether the value of the pixel is closer to VH than to M, then it is classified as a tumor and vice versa.

$$F1 = \begin{cases} 255 & \text{if } 0.5 T < X < 0.75 T \\ 0 & \text{if } X > 0.75 T \end{cases} \quad (10)$$

$$F2 = \begin{cases} 0 & \text{if } 1.5 T < X < 1.75 T \\ 255 & \text{if } X > 1.75 T \end{cases} \quad (11)$$

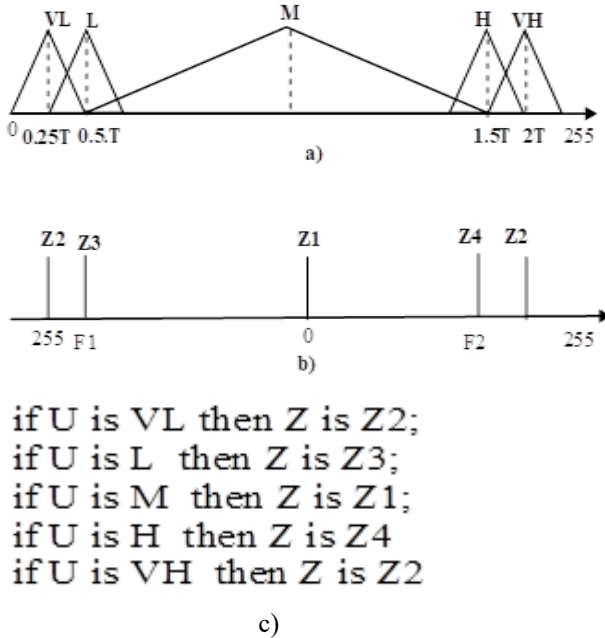


Figure 7. Specifications of the fuzzy inference module-2

D. Phase of brain tumor classification

The goal of this stage is to distinguish between four types of brain tumors (glioma tumors, meningioma tumors, no tumors, and pituitary tumors). The proposed technique for classifying the four different types of brain tumors is based on the use of CNN techniques. In the following, we will explain the technical specifications of the proposed CNN model.

1) Architecture of the planned CNN model

As shown in Figure 8, our suggested model (which is designed to classify brain tumors) includes three convolutional layers, three Max-pooling layers, one dropout layer, and a fully connected layer. The first convolutional layer (conv2D) receives an input image in

the size 150x150x3. This layer is made up of 16 filters with a 3x3 pixel size. The second one is made up of 64 filters with a 3x3 pixel size, and the third convolutional layer is made up of 128 filters with a 3x3 pixel size. These layers receive the output from the first layer. Following each one of the convolutional layers, an activation function is applied to the output after the convolution procedure to accommodate non-linearity. In our proposal, the ReLU activation function activates the convnet. Following the activation function is the sub-sampling layer, which uses a Max-pool with a 2x2 pixel size. Following the second and third sub-sampling layers is the dropout layer, which is a layer that is a regularization method for neural networks in which certain neurons are assigned at random and not used while retraining. Finally, there are three dense layers that discriminate between various brain tumor classes; these dense layers are with 'Softmax' activation function.

2) Hyper-parameters tuning of our suggested CNN model

Different sets of hyperparameters are required for different databases to produce accurate forecasts. The total amount of neurons for each layer, the activation function, the optimizer model, the batch size, the epochs (number of training iterations), the number of layers, the kernel size in convolutional layers, and the pooling size are typically the hyperparameters used to tune the deep conventional neural network. The validation set was used to address the following hyper-parameters in our proposed CNN model: Three convolutional layers include filters in different sizes (16, 64, and 128) all with 3x3 kernel size; then, three max-pooling layers include 2x2 kernel size, 64 neurons in each layer, ReLU activation function, Adam optimizer, 0.15 dropout rate, batch size at 16, epochs at 10, and one quantity of zero padding, all dedicated to a 0.001 learning rate. The loss function associated with the current model is the MAE loss. It is calculated by the following mathematical functions:

$$MAE = \frac{1}{N} \sum_{i=1}^N |Y_i - \bar{Y}_i| \quad (12)$$

Where,

N is the number of samples \bar{Y}_i is the predicted value, Y_i is the original value.

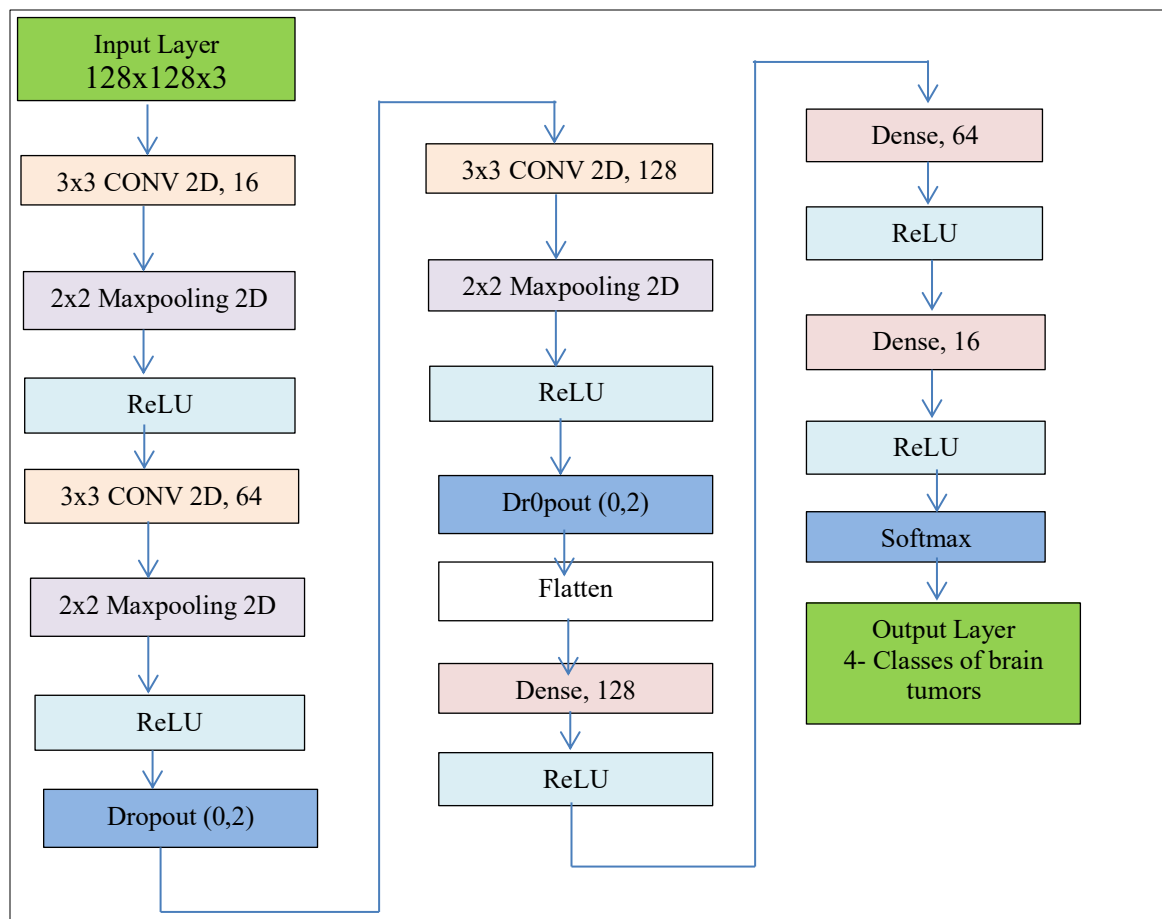


Figure 8. The architecture of the designed CNN algorithm.

IV. RESULTS AND DISCUSSION

In this section, the results of the proposed study for extracting and classifying brain tumors are reviewed. Therefore, the presentation of the results was divided into two parts. In the first part, the results of testing the accuracy of the proposed technique will be presented (compared to the results of other techniques) in extracting the tumor, and then calculating the size of the tumor. In the second section, the results of testing the accuracy of the proposed method will be presented (compared to the results of other techniques) for classifying the tumor into four different types. This is achieved through quantitative and visual evaluations and comparing the K-means clustering results, fuzzy C-means results, and the suggested method. Secondly, the training and evaluation achievements of the proposed brain tumor classification technique are analyzed, and the findings of the proposed approach are compared with other relevant processes. These results will be looked at below.

A. RESULTS OF BRAIN TUMOR EXTRACTION

To ensure the accuracy of the proposed brain tumor extraction method, two evaluation approaches were employed: quantitative analysis and visual assessment. In the following, we review the results evaluating the proposed

method compared to the results of related techniques. In the first section, we review the results of the evaluation using vision measures. In this section, the results of comparing the accuracy results of the proposed method in extracting tumors from the brain mass are reviewed compared to the results of two related techniques (and fuzzy C-means clustering K-means). In the second section of the review of brain tumor extraction results, two quantitative evaluation measurements are used (*dice* similarity coefficient index, confusion matrix, and effectiveness measures).

1) VISION ASSESSMENTS

Table 5 shows the outcomes of the proposed algorithm used to extract brain tumors in comparison to the outcomes of K-means clustering and fuzzy C-means clustering algorithms. The efficiency of each technique was evaluated based on its ability to accurately extract all heterogeneous regions within the brain mass. Therefore, the technique most capable of extracting these regions completely and without loss, without looking at the rest of the brain mass region (natural regions), will be considered the technique with the highest efficiency. In the results, the extracted areas appear in white, and anything below that appears in black. Looking at the results obtained, it appears that they are the results of different MRI image samples, some of which contain more than one heterogeneous spot, some of which contain one spot, and some of which do not contain heterogeneous areas.

Looking at the results of the three techniques, it is evident that the proposed technique has a great ability to extract various stains compared to the results of other techniques. The results demonstrate a remarkable ability to extract heterogeneous regions, regardless of their size. On the other hand, the results show a great similarity between the results of the K-Means and fuzzy C-Means techniques and their work methodology. We also note the difficulties that these techniques face in extracting more than one type of stain. The results also demonstrate that the proposed technique successfully avoids extracting any spots from images that do not contain tumors, a result not achieved by the other methods. In contrast, when analyzing images of healthy individuals completely free of heterogeneous regions, the efficiency of the technique is confirmed by the absence of any lines or white spots in the output.

2) QUANTITATIVE EVALUATION MEASURE

Quantitative analysis is expected to give a useful assessment of the difference in precision between the proposed strategy and other traditional techniques. The research effort that was put forward included two distinct quantitative evaluation techniques: dice similarity coefficient index and confusion matrix and effectiveness measurements. We examine the results of the quantitative review using the previously explained strategies in what follows to ascertain the superior performance of the technique used in classifying brain tumors in comparison to other related approaches, remembering the care that was used in choosing the appropriate approaches to ensure that they weren't data-slowing techniques.

2.1) INDEX OF DICE SIMILARITY COEFFICIENT

The Dice score is frequently used in regard to image division to determine how comparable the proposed segmentation mask is to the ground truth segmentation mask [41]. Complete overlap is represented by a score of 1, while no overlap is represented by a score of 0. To compute the dice similarity coefficient index, use the next analytical function, which is shown in the following:

$$d = 2 * \frac{|R_{seg} \cap R_{gt}|}{|R_{seg}| + |R_{gt}|} \quad (13)$$

In this case, R_{gt} denotes the ground truth segmentation mask, and R_{seg} is the segmentation outcome of the suggested procedure.

Table 7 displays the findings of an analysis of brain tumor extraction using three techniques: the K-Means algorithm, the fuzzy C-Means, and the proposed algorithm. The results of testing the accuracy of the proposed method for extracting areas believed to be tumors compared to the results of related techniques show a significant superiority in favor of the proposed technique, as shown in Table 8. The average efficiency of the proposed method on samples of images,

which were randomly selected from the database, reached 97.97%, while the other techniques achieved a much lower average efficiency (fuzzy C-Means achieved 69.37%, and K-Means achieved 66.65%). It is also noted that the results of traditional techniques are very similar. It is noteworthy that these techniques (K-Means and fuzzy C-Means) were chosen because they are among the most commonly used techniques for clustering images. It is also mentioned that the Otsu technique was tested until its results were completely poor, so we did not take it into consideration. It is noteworthy that the results of testing the Yolo8 algorithm for identifying brain tumors ranged (in many previous studies) between 92% and 94% [40]. This indicates the importance of the study presented in this work.

2.2) CONFUSION MATRIX AND EFFECTIVENESS MEASURES

The confusion matrix, also known as the mistake matrix, is generally used for quantifiable segmentation. A specific table layout allows one to visualize the effectiveness of an approach. In the data matrix, a row denotes a particular case of a predicted value, while the column indicates the actual quantity or the reverse. The outcome matrix consists of four cells, which are true positive (TP), false positive (FP), false negative (FN), and true negative (TN). The symbols shown below represent several cases: In terms of the model's estimation predicted result, TP indicates a positive value for every one of the real and predicted values; TN indicates a positive value corresponding to the actually however unfavorable outcome; FP indicates a negative value for the really however favorably expected value of the model; and FN indicates an unfavorable value for both the actual and predicted values. In this instance, the MRI image is split into two regions: the homogeneous areas (free of tumors) were considered the negative zone, and heterogeneous areas (expected to be tumors) were considered the positive zone. The tables from 9 to 11 display the findings of the confusion matrix for the suggested algorithms, K-means- clustering, and fuzzy C-means algorithms. The results confirmed the superiority of the planned algorithm over the K-means and fuzzy C-means algorithms. The results show the efficiency of the proposed technique to distinguish between brain tumors and the rest of the natural brain mass, where it achieved an average efficiency of brain tumor detection of 97% and an average efficiency of removing the healthy area of 95%. On the other hand, it seems quite clear that the difficulties faced by both K-means and fuzzy C-means algorithms in extracting tumor areas or in getting rid of healthy areas and not showing them. In contrast, the fuzzy C-means technique achieved an efficiency of 76.5% in extracting tumor areas while it achieved an efficiency of 69.5% in removing healthy areas. The K-Means technology attained an efficiency of 75.5% to extract the tumor and 67.5% to get rid of the healthy areas.

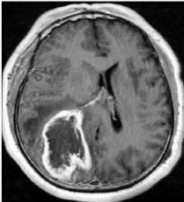


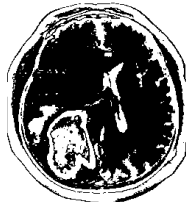
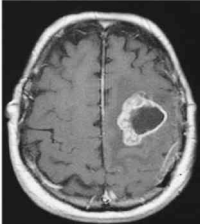


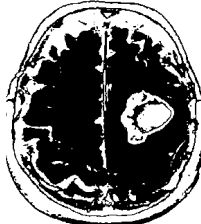

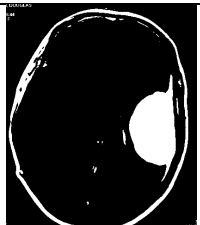
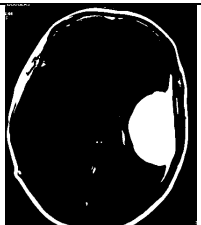

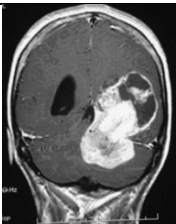



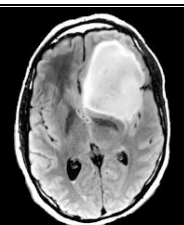



2.3) COMPUTATION OF DEFECTED REGIONS

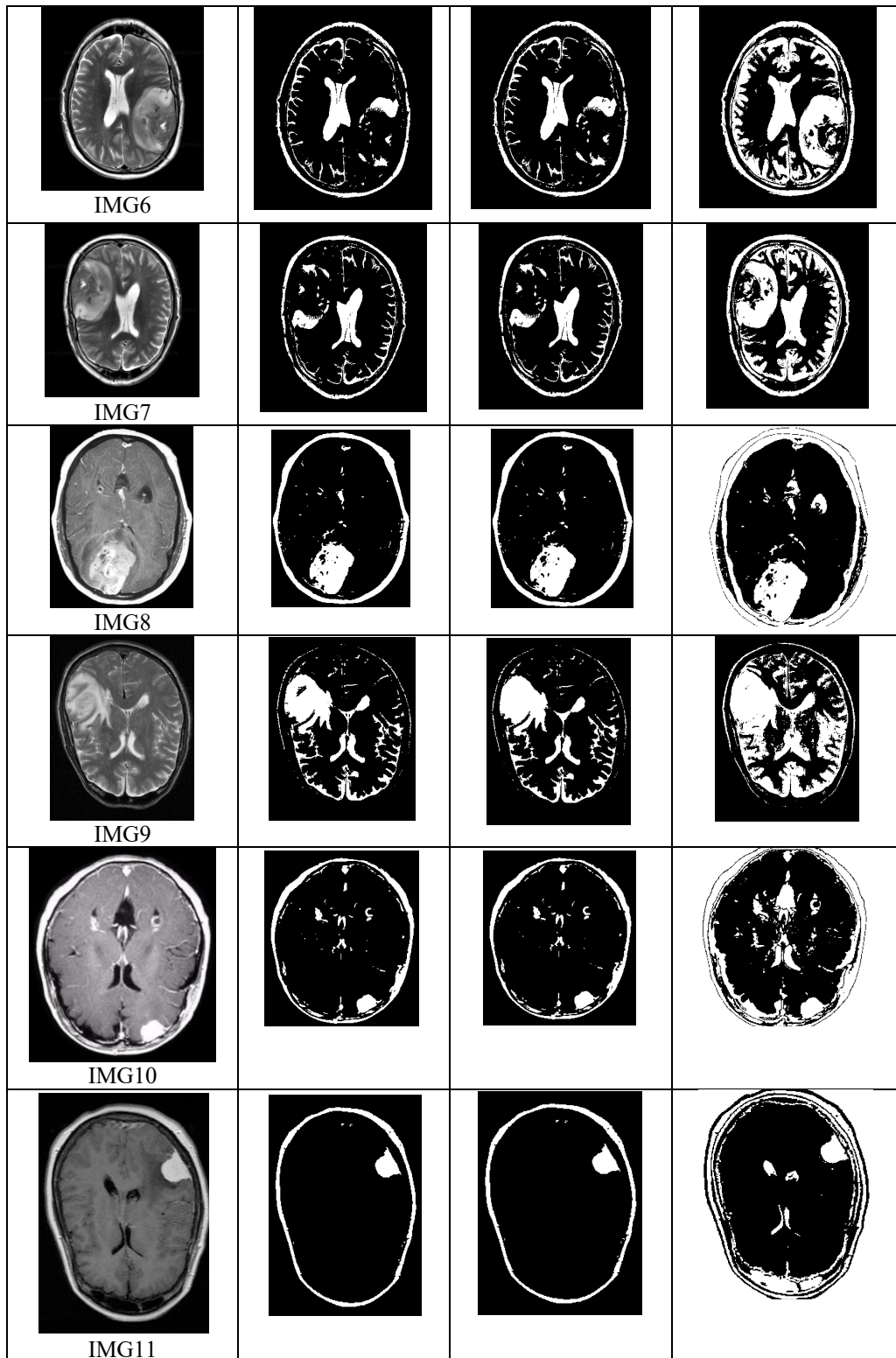
This section presents a comparison between the results of the proposed method for calculating the percentage of the total brain tumor size compared to the size of the entire brain mass

with the results of related techniques (K means and fuzzy C means). The comparison between the results of the proposed method and related techniques for calculating the percentage of tumor volume for ten samples of brain tumor MRI images, which are presented in Table 12, shows great superiority in favor of the proposed method. The results show the high

ability and flexibility of the proposed method to extract any spot that is not homogeneous with the rest of the brain mass, regardless of the size and diversity of those spots, which is not achieved with other techniques.

TABLE 7
OBTAINED RESULTS BY PROPOSED APPROACH FOR BRAIN TUMOR DETECTION COMPARED TO K-MEANS AND FUZZY C-MEANS ALGORITHMS IN SELECTED SAMPLES OF MRI BRAIN TUMOR IMAGE

Original image	K-Means Clustering	Fuzzy C-Means	Proposed Method
 IMG1			
 IMG2			
 IMG3			
 IMG4			
 IMG5			



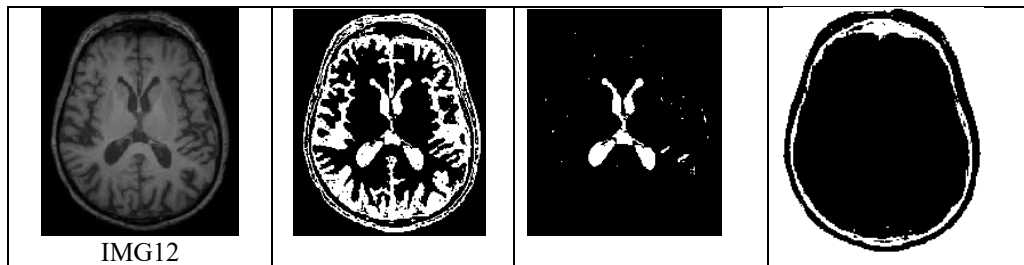
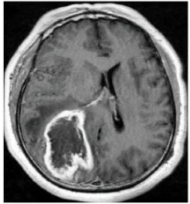
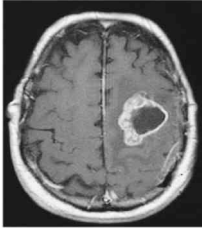
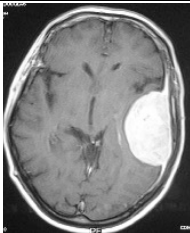
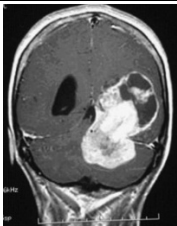
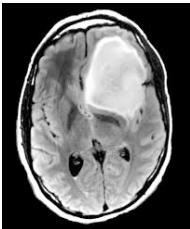
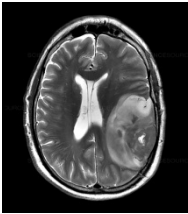
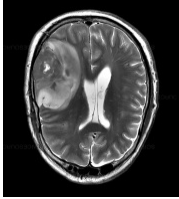
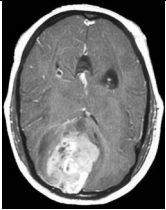
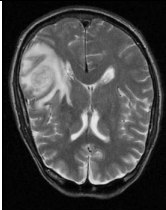
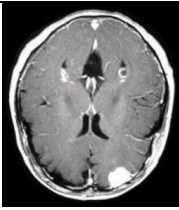
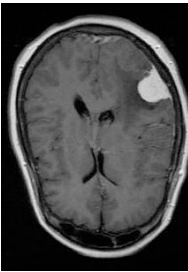
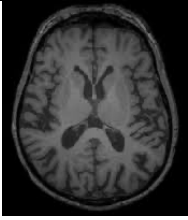


TABLE 8

OBTAINED RESULTS OF DICE COEFFICIENTS OF THE PROPOSED ALGORITHM AND SELECTED CONVENTIONAL ALGORITHMS

Original image	K-Means Clustering	Fuzzy C-Means	Proposed Method
 IMG1	0.6687	0.6732	0.9798
 IMG2	0.6065	0.6165	0.9896
 IMG3	0.9160	0.9232	0.9994
 IMG4	0.7456	0.7645	0.9843
 IMG5	0.6284	0.6420	0.9932

 IMG6	0.6720	0.6881	0.9464
 IMG7	0.6258	0.6460	0.9357
 IMG8	0.8702	0.7967	0.9967
 IMG9	0.8430	0.8627	0.9495
 IMG10	0.5427	0.5223	0.9932
 IMG11	0.7202	0.7491	0.9988
 IMG12	0.3421	0.4200	1.00

# Overall Accuracy	0.6665	0.6937	0.9797
--------------------	--------	--------	--------

TABLE 9
RESULTS OF THE CONFUSION MATRIX OF THE PROPOSED ALGORITHM

Predicted Value		Actual Value		Total Accuracy
		Accuracy of True Positive (TP)	Accuracy of false positive (FP)	100%
	Positive	94%-100% Average = 97%	0%-6% Average = 3%	
	Negative	Accuracy of False Negative (FN)	Accuracy of True Negative (TN)	100%
		2%-8% Average = 5%	92%-98% Average = 95%	

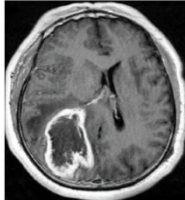
TABLE 10
RESULTS OF THE CONFUSION MATRIX OF THE FUZZY C-MEANS ALGORITHM

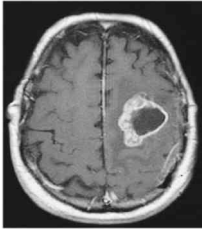
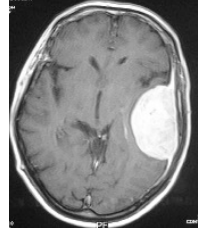
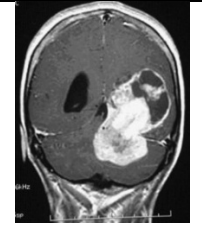
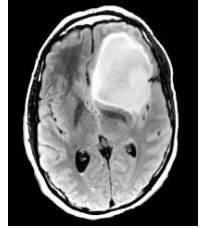
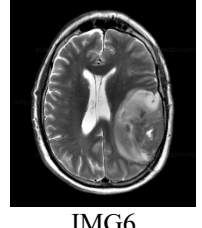
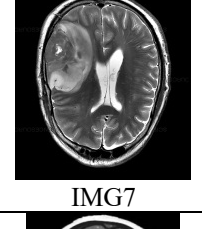
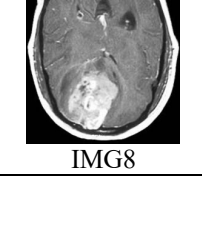
Predicted value		Actual Value		Total Accuracy
		Accuracy of True Positive (TP)	Accuracy of false positive (FP)	100%
	Positive	61%-92% Average = 76.5%	8%-39% Average = 23,5%	
	Negative	Accuracy of False Negative (FN)	Accuracy of True Negative (TN)	100%
		22%-39% Average = 30.5 %	61%-78% Average = 69.5%	

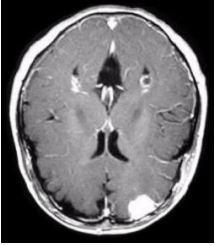
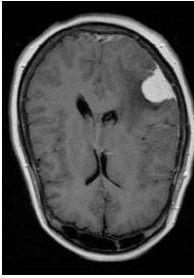
TABLE 11
RESULTS OF THE CONFUSION MATRIX OF THE K-MEANS ALGORITHM

Predicted value		Actual Value		Total Accuracy
		Accuracy of True Positive (TP)	Accuracy of false positive (FP)	100%
	Positive	60%-91% Average = 75.5%	9%-40% Average =24.5%	
	Negative	Accuracy of False Negative (FN)	Accuracy of True Negative (TN)	100%
		21%-45% Average = 33 %	55%-79% Average = 67%	

TABLE 12.
SIZE OF BRAIN TUMORS IN SELECTED BRAIN TUMOR MRI IMAGES

Original image	K-Means Clustering	Fuzzy C-Means	Proposed Method
 IMG1	5.2%	5.3%	27.23%

 IMG2	8.12%	8.12%	12.56%
 IMG3	15.21%	15.21%	18.67%
 IMG4	21.23	22.42	36.45%
 IMG5	22.92	23.34%	46.12%
 IMG6	17.89%	18.22%	47.32%
 IMG7	15.55%	16.98%	46.11%
 IMG8	21.11%	21.43%	27.87%

 <p>IMG9</p>	9%	9.11%	18.25%
 <p>IMG10</p>	5%	5%	10.23%

B. RESULTS OF BRAIN TUMOR CLASSIFICATIONS

In this section, the results of training, validation, and testing of the proposed technique for classifying brain tumors are reviewed. The results include the following: first, the results of training the proposed technology; second, the results of verifying the quality of the proposed technology; and third, the results of testing the accuracy of the proposed technology through the use of the Confusion Matrix mechanism. The results are supplemented by comparisons between the results of testing the proposed technology and related technologies.

1) TRAINING AND VALIDATING RESULTS OF THE SUGGESTED MODEL

Using 9904 MRI brain tumor images from the first database (these images are categorized into four groups based on the database description for each category), 27604 MRI images from the second database, and 32040 images from the third and final database, the proposed technique was trained. 1576 MRI brain tumor images from the first database (divided into four categories according to what was mentioned in the database description), 5244 MRI images from the second database, and 10684 images from the third database were used to verify the efficiency of the proposed technique.

One of the outcomes is training accuracy, which shows how well the model absorbs the training data. Validation accuracy shows how well the model generalizes to new data. F1-score, precision, and recall: To evaluate the suggested algorithm's overall classification performance for every dataset, these metrics would be helpful. Loss, the last metric, assesses how well the model reduces training and validating errors. The following provides an explanation of the outcomes obtained: First, the training results show that the model correctly classified the images in the first dataset's training set with an accuracy of 98.22%, the second dataset's training set with an accuracy of 98.66%, and the third dataset's training set with an accuracy

of 99%. This shows that the model has mastered the ability to differentiate between the four types of brain tumors in humans for each one of the three datasets. Based on the precision metrics provided in Figures 9 and 10 for training and validating the proposed algorithm to classify the images into four classes in each dataset, the proposed model appears to be performing exceptionally well. The model correctly identified 98.1% of the first dataset, 99.4% of the second dataset, and 99.4% of the third one. Images in the second and third datasets have a high precision of 99.4% indicating excellent performance in classifying the four types of brain tumors. It is not much different in the first dataset, where the proposed technique achieved 98.1%. Based on the recall results, the model is performing exceptionally well in identifying the four classes. The average of what the proposed technique achieved after training and validation was 98% for identifying the four classes of data in the three databases. This indicates the great ability that the proposed technique has acquired after training on this amount of images that were obtained from different sources. The situation is essentially the same in the F1score results, where the technique's average score across the three training datasets was 98.65. Conversely, the average F1 score of validation for the three databases designated for validation was 98.28%. This confirms the great ability that the proposed technique acquired in identifying the four different types of brain tumors, due to training on this huge amount of images. A low loss of 0.04 (which is achieved by the proposed model) indicates that the model is learning effectively and producing accurate predictions.

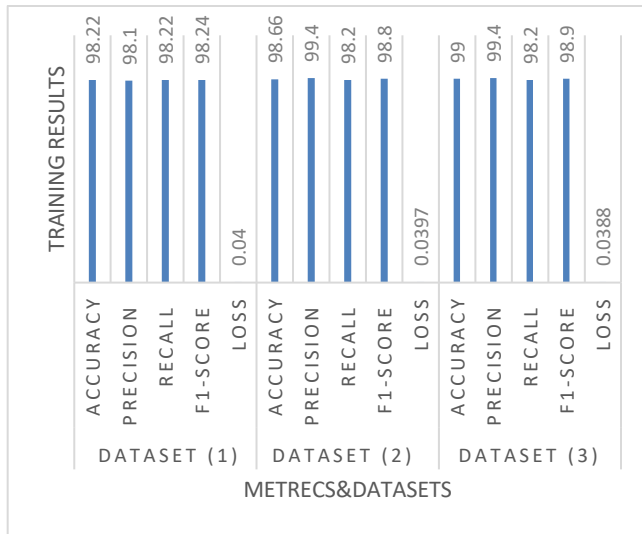


Figure 9. Performance of training results of the proposed method over the three datasets.

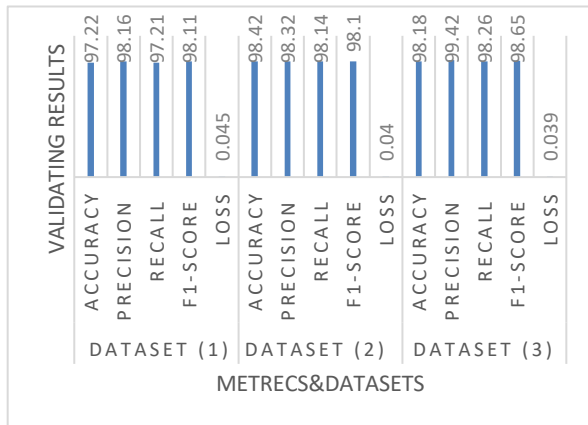


Figure 10. Performance of validating results of the proposed method over the three datasets.

Table 13 contains the training and validating time results of the proposed method. An encouraging sign is that the model's inference speed stays constant during training and validation. Each image is processed in under 10 milliseconds, which makes it perfect for real-time systems. In medical imaging, where it is essential to classify several images quickly and accurately, this speedy processing is very significant. The model's efficiency in classification is demonstrated by the consistent time spent during training and validation.

TABLE 13
TRAINING AND VALIDATING TIME RESULTS OF THE PROPOSED METHOD

Metric	Training time/image	Validation time/image
Total Inference Time	10ms	10ms

2) CONFUSION MATRIX FOR TESTING THE PROPOSED CLASSIFIER

Two quantitative measures, namely sensitivity and precision, have been used to evaluate the classification efficiency. The sensitivity is the capacity to identify a single occurrence of certain categories among the supplied data. The percentage of true positive categories that are accurately identified is what matters. On the other hand, precision is defined as the percentage of correctly identified positive predictions among all predicted positive cases. The formulas of the two measures are depicted below:

$$Sensitivity = \frac{TP}{(TP + FN)} \quad (14)$$

$$Precision = \frac{TP}{(TP + FP)} \quad (15)$$

The predictions for true positive, false positive, and false negative for the categories under consideration are denoted by the signs TP, FP, and FN.

The effectiveness of the proposed method was tested using 1576 MRI brain tumor images from the first database, 5244 MRI images from the second database, and 10684 images from the third database.

Table 14 shows the results of testing the proposed technique on the first database. The total number of images used from the first database to test the proposed technique is 1576 images distributed over the four categories as follows: 400 for the first category, 460 for the second category, 420 for the third category, and 296 for the last category.

The results show that the proposed technique recognized the second type of human brain tumor (Meningiomas) with a very high efficiency of 99%. The proposed technique achieved a 97% accuracy in recognizing the first type of tumor. Despite the significant similarity between the images of the third and fourth tumor types, it maintained an excellent accuracy of 96% in distinguishing between them. The average efficiency of the proposed technique in identifying the type of cancerous brain tumor for the four types from the first database reached 97%. These results reflect and confirm the high efficiency of the proposed technique in the ability to diagnose four different types of human brain tumors.

TABLE 14
RESULTS OF THE OVERALL ACCURACY OF TESTING THE PROPOSED ALGORITHM OVER THE FIRST DATASET

Actual class	Predicted class				Class sensitivity
	Glioma	Meningiomas	No Tumors	Pituitary Tumors	
Glioma	388	0	5	7	97%
Meningiomas	1	456	0	3	99%
No Tumors	8	0	403	9	96%

Pituitary Tumors	9	0	3	284	96%
Class Precision	96%	100%	98 %	94%	Overall correctn ess= 97%

Table 15 shows the results of testing the proposed technique on 5244 MRI images, which were allocated to test the proposed technique from the second database. These images are distributed over the four classes as shown in the table. The results show that the proposed technique achieved 99% in identifying the second class, 98% in identifying the first and third classes, and 97% in identifying the fourth class. The results indicate that the proposed technique recognized the four classes from the second database better than from the first database, as the average efficiency of testing the proposed technique to classify the four classes of brain tumors reached 98% compared to 97% on the first database. The results generally indicate a great ability of the proposed technique to classify and diagnose four classes of human brain tumors.

TABLE 15
RESULTS OF THE OVERALL ACCURACY OF TESTING THE PROPOSED ALGORITHM OVER THE SECOND DATASET

Actual class	Predicted class				Class sensitivity
	Glioma	Meningiomas	No Tumors	Pituitary Tumors	
Glioma	1188	0	5	7	98%
Meningiomas	5	1212	0	7	99%
No Tumors	14	0	1588	18	98%
Pituitary Tumors	22	0	14	1164	97%
Class Precision	96%	100%	98 %	94%	Overall correctn ess= 98%

Table 16 shows the results of testing the proposed technique on 9684 MRI images, which were allocated to test the proposed technique from the third database. These images are distributed among the four categories as shown in the table. The obtained results show that the proposed technique achieved 99% accuracy in identifying the second type of brain tumor and 98% accuracy in identifying the remaining types of tumors. The proposed technique demonstrated superior performance in classifying the four types of brain tumors when tested on the image samples from the third database, achieving an average classification accuracy of 98.25%, which outperformed the results obtained from the first and second databases. These findings further confirm

the high capability of the proposed method in accurately identifying human brain tumors.

TABLE 16
RESULTS OF THE OVERALL ACCURACY OF TESTING THE PROPOSED ALGORITHM OVER THE THIRD DATASET

Actual class	Predicted class				Class sensitivity
	Glioma	Meningiomas	No Tumors	Pituitary Tumors	
Glioma	3116	0	20	44	98%
Meningiomas	8	2606	2	16	99%
No Tumors	12	0	980	8	98%
Pituitary Tumors	46	0	11	2815	98%
Class Precision	96%	100%	98 %	94%	Overall correctn ess= 98%

3) COMPARISON WITH THE RELATED DEEP LEARNING TECHNIQUES

This section compares the average results of twelve related deep learning techniques with the average results of the suggested technique's accuracy test in identifying the four types of brain tumors over the three databases used in this study. Tables 17 and 18 display the outcomes of an analysis of the test accuracy of the proposed method with twelve comparable DL strategies to categorize brain tumors into four groups. The accuracy of the proposed technique was tested against deep learning techniques on 16504 MRI brain tumor images collected from the three databases used in this study. These images are divided into the four types of brain tumors as follows: 4280 images for the first class, 4316 for the second class, 3040 for the third class, and 4368 for the last class. The obtained results highlight the excellent performance of the proposed technique in terms of precision. Compared to other methods, it demonstrates a higher ability to provide correct positive predictions, achieving a precision of 98%. In contrast, other techniques recorded lower precision values, ranging from 88% for MobileNetV2 to 94% for the Vision Transformer (ViT). The proposed technique also achieved the highest F1 score of 98.32%, much higher than other techniques whose values ranged from 84% for VGG16 to 93% for EfficientNetB7, reflecting its balanced performance. On the other hand, at 10 ms, the speed achieved by the proposed technique indicates that it is much faster than other models, as it is faster than heavyweight models such as EfficientNetB7 (114 ms) and DenseNet201 (62 ms) by 6 to 10 times. It is also faster than lightweight models such as MobileNetV2 (11 ms) and

ResNet50 (11 ms). The Model's FPR of 0.0398% is the lowest among all the models, indicating its reliability in avoiding errors. The results show that the proposed model is compact and efficient compared to all other models, and the proposed model achieves a balance between computational complexity and performance, outperforming all other models. The proposed model outperforms all other models in terms of accuracy, f1 score and recall, which are very important metrics for medical image classification. Despite its high accuracy, the proposed model maintains excellent inference time (10 ms) and small size (14 MB), which makes it very suitable for real-time applications.

TABLE 17
COMPARISON OF THE PROPOSED ALGORITHM'S TEST ACCURACY SCORES
WITH THOSE OF RELATED DEEP LEARNING ALGORITHMS

model	Precision	F1-Score	Inference time ms
MobileNetV2	0.88	0.85	11
EfficientNetB0	0.88	0.85	14
EfficientNetB4	0.92	0.90	42
EfficientNetB7	0.93	0.92	114
ResNet50	0.88	0.89	10
ResNet101	0.90	91	42
VGG16	0.85	0.84	25
VGG19	0.89	0.87	41
InceptionV3	0.91	0.91	32
DenseNet121	0.92	0.92	41
DenseNet201	0.92	0.93	62
Vision Transformer (ViT)	0.94	0.91	63
Proposed Model	0.98	0.9832	10

TABLE 18
COMPARISON OF THE PROPOSED ALGORITHM'S TEST ACCURACY SCORES
WITH THOSE OF RELATED DEEP LEARNING ALGORITHMS

model	FPR	Model size MB	Recall
MobileNetV2	0.150	15	0.86
EfficientNetB0	0.132	22	0.87
EfficientNetB4	0.062	78	0.93
EfficientNetB7	0.063	256	0.94
ResNet50	0.092	102	0.90
ResNet101	0.078	174	0.92
VGG16	0.151	532	0.85
VGG19	0.142	552	0.87
InceptionV3	0.052	97	0.91
DenseNet121	0.078	31	0.91

DenseNet201	0.049	84	0.92
Vision Transformer (ViT)	0.059	25	0.93
Proposed Model	0.0398	14	98.32

V. CONCLUSION AND FUTURE WORKS

This study presents an efficient approach for brain tumor detection and classification by integrating fuzzy logic with DL techniques. The proposed method demonstrates significant improvements in accuracy and computational cost compared to traditional and state-of-the-art approaches. Experiments have been conducted on three public datasets showing that the proposed model performs well across various brain tumor types, including gliomas, meningiomas, and pituitary tumors. With a classification accuracy of 98% and a Dice similarity coefficient of 97.97%, our results underline the robustness and reliability of combining fuzzy logic with DL. In addition, the proposed approach was able to precisely calculate tumor size, which offers detailed insights into tumor severity and progression.

Future work will focus on implementing the proposed framework in hardware systems to further optimize its real-time capabilities and integration into medical imaging workflows. The proposed system can be implemented on a low-cost FPGA from the Spartan-3 Xilinx family. The circuit is expected to occupy approximately 300 slices, corresponding to an estimated cost of 5,450 equivalent gates. It can operate at a frequency of 80 MHz, with an expected processing time of 0.339 ms per image, enabling the system to process approximately 3,000 images per second. Another direction for future work involves developing a system capable of extracting and visually distinguishing each type of brain tumor within MRI images, thereby enhancing interpretability and diagnostic clarity. Additionally, establishing collaboration agreements with hospitals and clinical research centers is planned to validate the proposed method on real-world MRI datasets. These findings reflect a promising step toward enhancing automated brain tumor diagnostics, improving patient outcomes, and advancing AI-driven healthcare solutions.

Data availability

The dataset used in this study is available online for free at <https://www.kaggle.com/datasets/sartajbhuvaji/brain-tumor-classification-mri> and <https://www.kaggle.com/datasets/masoudnickparvar/brain-tumor-mri-dataset>

Conflicts of Interest

The authors have no conflicts of interest to declare.

Acknowledgments

The authors would like to acknowledge the support of Prince Sultan University for paying the Article Processing Charges (APC) of this publication.

REFERENCES

- [1] Ganesh D. Barkade, Pranjal S. Bhosale, Sakshi K. Shirsath, "Overview of brain cancer, its symptoms, diagnosis and treatment", *IP International Journal of Comprehensive and Advanced Pharmacology*, pp:159–164, v. 8, 2023, DOI: 10.18231/j.ijcaap.2023.027.
- [2] Demyana A. Saleeb; Rehab M. Helmy; Nihal F. F. Areed; Mohamed Marey; Wazie M. Abdulkawi; Ahmed S. Elkorany, "A technique for the early detection of brain cancer using circularly polarized reconfigurable antenna array", *IEEE ACCESS*, 2021, Vol.9, pp.133786-133794, DOI: 10.1109/ACCESS.2021.3115707.
- [3] Hammad, M., ElAffendi, M., Ateya, A.A. and Abd El-Latif, A.A., 2023, "Efficient brain tumor detection with lightweight end-to-end deep learning model", *Cancers* 2023, MDPI, Vol.15, p.p:1-16, DOI: 10.3390/cancers15102837.
- [4] Rao CS, Karunakara K. "Efficient Detection and Classification of Brain Tumor using Kernel based SVM for MRI" *Multimedia Tools and Applications*. 2022 Jan 26, Vol.81, p.p:7393-7417, DOI:10.1007/s11042-021-11821-z.
- [5] M. M. Badz'a and M. C'. Barjaktarovic, "Classification of brain tumors from mri images using a convolutional neural network" *Applied Sciences* 2020, vol.10, p.p:1-13, DOI: <https://doi.org/10.3390/app10061999>.
- [6] Alyami, J., Rehman, A., Almutairi, F., Fayyaz, A.M., Roy, S., Saba, T. and Alkhurim, A., "Tumor localization and classification from MRI of brain using deep convolution neural network and Salp swarm algorithm", *Cognitive Computation* 2024, Vol.16, pp.2036-2046, DOI: 10.1007/s12559-022-10096-2
- [7] Cheng, J.; Huang, W.; Cao, S.; Yang, R.; Yang, W.; Yun, Z.; Wang, Z.; Feng, Q. "Enhanced Performance of Brain Tumor Classification via Tumor Region Augmentation and Partition", *PLoS ONE* 2015, Vol.10, pp:1-22, DOI: 10, e0140381.
- [8] Zahid Rasheed, Yong-Kui Ma, Inam Ullah, Yazeed Yasin, Ghadi, Muhammad Zubair Khan, Muhammad AbbasKhan, Akmalbek Abdusalomov, Fayeze Alqahtani, Ahmed M Shehata, "Brain Tumor Classification from MRI Using Image Enhancement and Convolutional Neural Network Techniques", *Brain Sci.* 2023 Sep 14; Vol.13, pp:1-22. doi: 10.3390/brainsci13091320
- [9] M. Ravinder, Garima Saluja, Sarah Allabun, Mohammed S. Alqahtani, Mohamed Abbas, Manal Othman & Ben Othman Soufiene, "Enhanced brain tumor classification using graph convolutional neural network architecture, *Scientific Reports* 2023, Vol.13, pp:1-22, DOI: | <https://doi.org/10.1038/s41598-023-41407-8>.
- [10] Varone, G., Boulila, W., Lo Giudice, M., Benjdira, B., Mammone, N., Ieracitano, C., Dashtipour, K., Neri, S., Gasparini, S., Morabito, F.C. and Hussain, A., "A machine learning approach involving functional connectivity features to classify rest-EEG psychogenic non-epileptic seizures from healthy controls", *Sensors* 2021, Vol.22, p.129, DOI:10.3390/s22010129.
- [11] Varone, G., Boulila, W., Driss, M., Kumari, S., Khan, M.K., Gadekallu, T.R. and Hussain, A., "Finger pinching and imagination classification: A fusion of CNN architectures for IoMT-enabled BCI applications". *Information Fusion* 2024, Vol.101, p.102006, DOI: <https://doi.org/10.1016/j.inffus.2023.102006>
- [12] Kotte Sowjanya , Munazzar Ajreen , Paka Sidharth , Kakara Sriharsha , Lade Aishwarya Rao, "Fuzzy thresholding technique for multiregion picture division", *International Research Journal on Advanced Science Hub*, Vol. 04, pp: 44-50, DOI: 10.47392/IRJASH.2022.011.
- [13] M. F. I. Soumik and M. A. Hossain, "Brain tumor classification with inception network based deep learning model using transfer learning," in *2020 IEEE Region 10 Symposium (TENSYP)*. IEEE, 2020, pp. 1018–1021, DOI: 10.1109/TENSYP50017.2020.9230618
- [14] Sasikala, M.; Kumaravel, N. "A wavelet-based optimal texture feature set for classification of brain tumours". *J. Med. Eng. Technol.* 2008, 32, 198–205, DOI:10.1080/03091900701455524.
- [15] El-Dahshan, E.-S.A.; Hosny, T.; Salem, A.-B.M., "Hybrid intelligent techniques for MRI brain images classification" *Digit. Signal Process Elsevier*, 2010, vol.20, pp:433–441, DOI: <https://doi.org/10.1016/j.dsp.2009.07.002>.
- [16] Kaplan, K.; Kaya, Y.; Kuncan, M.; Ertunc, H.M., "Brain tumor classification using modified local binary patterns (LBP) feature extraction methods", *Med. Hypotheses* 2020, vol.139, 109696, DOI: 10.1016/j.mehy.2020.109696.
- [17] Perri, R.L.; Castelli, P.; La Rosa, C.; Zucchi, T.; Onofri, "A. COVID-19, Isolation, Quarantine: On the Efficacy of for Ongoing Trauma", *Brain Sci.* 2021, vol.11, pp:1-8, DOI: <https://doi.org/10.3390/brainsci11050579>.
- [18] Mohsen, H.; El-Dahshan, E.-S.A.; El-Horbaty, E.-S.M.; Salem, A.-B.M., "Classification using deep learning neural networks for brain tumors. *Future Computing and Inform. J.* 2018, vol.3, pp:68–71, DOI: 10.1016/j.fcij.2017.12.001.
- [19] Cheng, J. Figshare Brain Tumor Dataset. 2017. Available online: https://figshare.com/articles/dataset/brain_tumor_dataset/1512427 (accessed on 13 May 2022).
- [20] Pashaei, A.; Sajedi, H.; Jazayeri, N., "Brain Tumor Classification via Convolutional Neural Network and Extreme Learning Machines", In *Proceedings of the 2018 8th International Conference on Computer and Knowledge Engineering (ICCCKE)*, Mashhad, Iran, 25–26 October 2018; pp. 314–319, DOI: DOI: 10.1109/ICCCKE.2018.8566571.
- [21] Phayé, S.S.R.; Sikka, A.; Dhall, A.; Bathula, D. "Dense and Diverse Capsule Networks: Making the Capsules Learn Better", *arXiv* 2018, arXiv:1805.04001, DOI: <https://doi.org/10.48550/arXiv.1805.04001>.
- [22] M. M. Badz'a and M. C'. Barjaktarovic, "Classification of brain tumors from mri images using a convolutional neural network" *Applied Sci- ences*, vol. 10, no. 6, p. 1999, 2020, DOI: <https://doi.org/10.3390/app10061999>
- [23] J. D. Bodapati, N. S. Shaik, V. Naralasetti, and N. B. Mundukur, "Joint training of two-channel deep neural network for brain tumor classification," *Signal, Image and Video Processing* 2021, vol. 15, no. 4, pp. 753–760, DOI: <https://doi.org/10.1007/s11760-020-01793-2>.
- [24] A. Rehman, S. Naz, M. I. Razzak, F. Akram, and M. Imran, "A deep learning-based framework for automatic brain tumors classification using transfer learning," *Circuits, Systems, and Signal Processing* 2020, vol. 39, no. 2, pp. 757–775, DOI: <https://doi.org/10.1007/s00034-019-01246-3>
- [25] S. Deepak and P. Ameer, "Brain tumor classification using deep cnn features via transfer learning," *Computers in biology and medicine* 2019, vol. 111, DOI: <https://doi.org/10.1016/j.combiomed.2019.103345>.
- [26] NVSL Narasimham, Keshav Kumar K. "Fuzzy Logic-Based System for Brain Tumour Detection and Classification", *arXiv*, vol.2401, pp:1-14, doi: <https://doi.org/10.48550/arXiv.2401.14414>.
- [27] Pham Van Hai, Samson Eloanyi Amaechi, "Convolutional Neural Network Integrated With Fuzzy Rules for Decision Making in Brain Tumor Diagnosis", *International Journal of Cognitive Informatics and Natural Intelligence*, Vol.15, pp:1-23 DOI: 10.4018/IJCINI.20211001.0a47, 2021.
- [28] Sarmad Maqsood , Robertas Damasevicius(B) ,and Faisal Mehmood Shah, "An Efficient Approach for the Detection of Brain Tumor Using Fuzzy Logic and U-NET CNN, Classification", *Lecture Notes in Computer Science*, Springer, Vol. 12953, pp. 105–118, DOI: https://doi.org/10.1007/978-3-030-86976-2_8, 2021.
- [29] Mantripragada Yaswanth Bhanu Murthy, Anne Koteswararao, and Melingil Sunil Babu, "Adaptive fuzzy deformable fusion and optimized CNN with ensemble classification for automated brain tumor diagnosis", *Biomedical Engineering Letters* 2022, Springer, Vol. 12 pp:37–58, DOI: <https://doi.org/10.1007/s13534-021-00209-5>.
- [30] Robin Gutsche, Carsten Lowis, Karl Ziemons, Martin Kocher, Garry Ceccon, Cl audio R_egio Brambilla, Nadim J. Shah, Karl-Josef Langen, Norbert Galldiks, Fabian Isensee, and Philipp Lohmann, "Automated Brain Tumor Detection and Segmentation for Treatment Response Assessment Using Amino Acid PET", the *journal of nuclear medicine*, Vol. 64, pp: 1594-1602, October 2023, doi: 10.2967/jnumed.123.265725.
- [31] Rafael Martinez, Del-Rio-Ortega, Javier Civit-Masot, Francisco Luna, Perejon ,2 and Manuel Dominguez-Morales, "Brain Tumor Detection Using Magnetic Resonance Imaging and Convolutional Neural Networks", *Big Data Cogn. Comput. MDPI*, 2024, Vol.8, pp:

- 1-17. Doi: 10.3390/bdcc8090123.
- [32] Vinod Kumar Dhakshnamurthy, Murali Govindan, Kannan Sreerangan, Manikanda Devarajan Nagarajan and Abhijith Thomas, "Brain Tumor Detection and Classification Using Transfer Learning Models", Eng. Proc.MDPI, 2024, Vol.62, PP: 1-8. Doi: 10.3390/engproc2024062001.
- [33] Md. Mahfuz Ahmed, Md. Maruf Hossain, Md. Rakibul Islam, Md. Shahin Ali, Abdullah Al Noman Nafi, Md. Faisal Ahmed, Kazi Mowdud Ahmed, Md. Sipon Miah, Md. Mahbubur Rahman, Mingbo Niu & Md. Khairul Islam, "Brain tumor detection and classification in MRI using hybrid ViT and GRU model with explainable AI in Southern Bangladesh", Scientific reports, 2024, Vol.14, pp:1-16, doi: /10.1038/s41598-024-71893-3.
- [34] Manali Gupta, Sanjay Kumar Sharma, and G. C. Sampada. "Classification of Brain Tumor Images Using CNN", Hindawi, Computational Intelligence and Neuroscience, Vol. 2023, pp:1-6, doi: 10.1155/2023/2002855.
- [35] Muhammad Aamir, Abdallah Namoun, Sehrish Munir, Nasser Aljohani, Meshari Huwaytim Alanazi, Yaser Alsahafi 5 and Faris Alotibi. "Brain Tumor Detection and Classification Using an Optimized Convolutional Neural Network", Diagnostics, MDPI 2024, Vol.14, pp: 1-19. doi.org/10.3390/diagnostics14161714.
- [36] <https://www.kaggle.com/datasets/sartajbhuvaji/brain-tumor-classification-mri>
- [37] <https://www.kaggle.com/datasets/masoudnickparvar/brain-tumor-mri-dataset>
- [38] <https://www.kaggle.com/datasets/sabersakin/brainmri/data>.
- [39] Abdullah Elen, Emrah Dönmez, "Histogram-based global thresholding method for image binarization", Optik Journal July 2024, ELSEVIER, Vol. 306, PP:1-20, doi: DOI:10.1016/j.ijleo.2024.171814
- [40] Rahma Satila Passa, Siti Nurmaini, Dian Palupi Rini, "YOLOv8 Based on Data Augmentation for MRI Brain Tumor Detection", Scientific Journal of Informatics Aug 2023, Vol. 10, pp: 1-8, doi: DOI: 10.15294/sji.v10i3.45361.
- [41] Jifeng Ning, Lei Zhang, David Zhang a Chengke Wu, "Interactive image segmentation by maximal similarity based region merging", Pattern Recognition Journal 2010, ELSEVIER Volume 43, Issue 2, February 2010, Pages 445-456, doi:<https://doi.org/10.1016/j.patcog.2009.03.004>



Wadii Boulila Wadii Boulila received his B.Sc. degree (First-Class Honours with Distinction) in Computer Science from the Aviation School of Borj El Amri in 2005, his M.Sc. degree in Computer Science from the National School of Computer Science (ENSI) at the University of Manouba, Tunisia, in 2007, and his Ph.D. in Computer Science through a joint program between ENSI and Télécom Bretagne, University of Rennes 1, France,

in 2012. He is currently a Professor of Computer Science and the leader of the RIOTU Laboratory at Prince Sultan University, Saudi Arabia. In addition, he serves as a Senior Researcher with the RIADI Laboratory at the University of Manouba and previously held the position of Senior Research Fellow with the ITI Department at the University of Rennes 1, France. Prof. Boulila has been the recipient of several prestigious awards, including the Best Young Researcher in Computer Science Award in 2021 from Beit El-Hikma, the Best Researcher Award from the University of Manouba in 2021, the Most Cited Researcher Award from the University of Manouba in 2022, and the Research Excellence Award as well as the Best Faculty Member for Most Impactful Research Output Award from Prince Sultan University. He has actively contributed to numerous research and industrial projects, with primary research interests spanning data science, computer vision, big data analytics, deep learning, cybersecurity, artificial intelligence, and uncertainty modeling. Prof. Boulila has served as a chair, reviewer, and technical program committee (TPC) member for many leading international conferences and journals. His work has garnered global recognition, and he has been named among the top 2% of scientists worldwide in his field by Stanford University. He is a Senior Member of IEEE, a Member of ACM and AAAI, and a Senior Fellow of the Higher Education Academy (SFHEA) in the U.K.

AUTHOR'S BIOGRAPHY



Nashaat M. Hussain Hassan was born in Quena, Egypt, in 1977. He received his B.Sc. in communication and electronics engineering from Al-Azhar University – Egypt in 2002. In 2005, he received his M.Sc. degree in communication and electronics engineering from (C.N.M.) National Center of Microelectronics, Seville University – Spain. In 2009, he received his Ph.D. in Digital Integrated Circuit Design for the Applications of Image processing from (C.N.M.) National Center of

Microelectronics, Seville University – Spain. In October 2019 he was promoted to the position of an Associate Professor position. Currently, he is working as an associate professor in the department of Electronics & Electrical communication, Faculty of Engineering, Fayoum University – Egypt. His research interest includes algorithms development (analysis, design and improvement) and full-cycle software & Hardware product development (Matlab, C, C++, VHDL, FPGA, and Xilinx). He can be contacted at nmh01@fayoum.edu.eg.